한국ITS학회논문지
제3권, 제2호 (2004. 9 · 12)
pp.85~93

A GaAs Micromachined Millimeter-wave Lowpass Filter Using Microstrip Stepped-Impedance Hairpin Resonator

Ju-Hyun Cho* Tae-Soon Yun* Tae-Jong Baek**
Baek-Seok Ko** Dong-Hoon Shin** Jong-Chul Lee*

Abstract

In this paper, microstrip stepped-impedance hairpin resonator (SIR) lowpass filter (LPF) by surface micromachining on GaAs substrate is suggested. This filter has the advantages of compact size, easy fabrication, and sharp cutoff frequency response. The new SIR LPF shows the 3 dB passband of dc to 33 GHz, the insertion loss of 0.82 dB, and the return loss of better than 17 dB up to 25.57 GHz. This filter is useful for many microwave system applications.

Key Words : RF MEMS, surface micromachining, SIR hairpin LPF, DAML structure.

1. Introduction

Recently, the development of RF passive devices using MEMS (MicroElectroMechanical Systems) technology is actively in progress. It takes advantage of possibility to make the device with very high frequency range by overcoming the construction problem in existing way. MEMS devices have high Q, low loss, and low dispersion, and can be integrated with active devices on the same substrate [1,2]. There are two kinds of MEMS technology. One is a bulk-micromachining in which the pattern is formed on membrane by etching process of the substrate and the other is a surface micromachining in which the structure is made on the air through etching process of the sacrificial layer [3].

In this paper, a new SIR LPF with aperture is suggested using GaAs surface micromachining in 30 GHz range. The microstrip line is elevated by the polyimide dielectric post using surface micromachining technique and then it has air-gapped area between the signal line and the ground metal. Hence, the substrate dielectric loss can be reduced because most of the electric field is confined in air region between the signal line and the ground, not in dielectric substrate. Therefore, the new low loss microstrip structure can be easily realized without the complex process such as via-hole and back metalization, Since the DAML structure is compatible with the conventional MMIC (monolithic microwave integrated circuit) tech-

* RFIC Education and Research Center, Kwangwoon University
** Millimeter-wave INnovation Technology research center (MINT), Dongguk University
† 논문접수일 : 2004년 9월 18일

nologies, it is possible to integrate the passive MEMS components on the active GaAs MMIC, which can make the cost lower and the size smaller with good performance [4].

Microstrip stepped-impedance hairpin resonators have many attractive features [5] and can be used in satellite, mobile phones, and other wireless communication system. The main advantages of the resonators are their compact size, easy fabrication, sharp cutoff frequency response, and wide stopband. Therefore, the resonators are widely used in the design of filters, oscillators, and mixers [6].

Small-size low-pass filters are frequently required in many communication systems to suppress harmonics and spurious signals. The conventional stepped-impedance and Kuroda-identity-stub low-pass filters only provide Butterworth and Chebyshev characteristics with a gradual cutoff frequency response. This type of filter needs more sections and causes to increase the size of the filter and insertion loss. A compact semilumped low-pass filter has been also proposed. However, the structure using lumped elements increases difficulties in fabrication [7].

The microstrip Stepped-Impedance Resonator (SIR) low-pass filter using aperture [8] and inter-digital capacitor (IDC) shows the advantage of high performance, low loss, compact size, and sharp cutoff frequency response.

In this paper, an equivalent-circuit model for the stepped-impedance hairpin resonator is described. SIR hairpin low-pass filter using aperture is adopted to suppress the second harmonic component, to achieve a broad stopband bandwidth, and to improve the return loss.

2. Analysis of the Stepped-Impedance Hairpin Resonator

Fig. 1 shows the basic layout of the stepped-impedance hairpin resonator. The stepped-impedance hairpin resonator consists of the single transmission line l_s and coupled lines with a length of l_c. Z_h is the characteristic impedance of the single transmission line l_s. Z_{0e} and Z_{0o} are the even-mode and odd-mode impedance, respectively of symmetric capacitance-loaded parallel coupled lines with a length of l_c. By selecting $Z_h > \sqrt{Z_{0e}Z_{0o}}$, and employing aperture on the ground plane, the size of the stepped-impedance hairpin resonator becomes smaller than that of the conventional hairpin resonator, which is an elliptic-function low-pass filter using microstrip SIR hairpin resonator. Also, the effect of the loading capacitance shifts the spurious resonant frequencies of the resonator from integer multiples of the fundamental resonant frequency. Also it reduces interferences from high-order harmonics.

The resonator structure to be considered here is shown in Fig. 1(a). The SIR is symmetrical and has two different characteristic impedance lines, Z_h and Z_l , of admittance Y_h and Y_l.

The admittance of the resonator from the open end, Y_i is given by

$$Y_i = jY_1 \frac{2(K\tan\theta_1 + \tan\theta_2)\cdot(K - \tan\theta_1\cdot\tan\theta_2)}{K(1-\tan^2\theta_1)\cdot(1-\tan^2\theta_2) - 2(1+K^2)\cdot\tan\theta_1\cdot\tan\theta_2} \quad (1)$$

Where K is the impedance ratio (=Z_l / Z_h). The resonance condition can be obtain from the following condition:

$$Y_i = 0. \quad (2)$$

From (1) and (2), the fundamental resonance condition can be expressed as

$$K = \tan\theta_1 \cdot \theta_2. \quad (3)$$

The relationship between θ_r and θ_1 is derived from (3) as

$$\tan\frac{\theta_r}{2} = \frac{1}{1-K}\left(\frac{K}{\tan\theta_1} + \tan\theta_1\right) (\text{when } K \neq 1) \quad (4)$$

$$\theta_r = \pi \qquad (\text{when } K \approx 1). \qquad (5)$$

When $K=1$, this corresponds to a uniform impedance line resonator.

The resonator length θ_r has the minimum value when $0 < K < 1$ and the maximum value when $K > 1$. This condition can be obtained by differentiating (4) by θ_1,

$$\frac{1}{1-K} \cdot (\tan^2\theta_1 - K) \cdot \sin^2\theta_1 = 0 \qquad (6)$$

$$\theta_1 = \tan^{-1}(\sqrt{K}) = \theta_2 \qquad (7)$$

The above equation is the condition that θ_r has the maximum or minimum value for constant K. For practical application it is preferable to choose $\theta_1 = \theta_2$ because the design equations can be simplified considerably. Therefore, in the following discussion, the SIR is treated as with $\theta_1 = \theta_2$ and (1) can be expressed as

$$Y_i = jY_2 \frac{2(1+K) \cdot (K - \tan^2\theta) \cdot \tan\theta}{K - 2(1+K+K^2) \cdot \tan^2\theta + K\tan^4\theta} \qquad (8)$$

With the resonance condition and the fundamental frequency f_0, the corresponding length, θ_0 is give by

$$\tan^{-1}\theta_0 = K \text{ or } \theta_0 = \tan^{-1}\sqrt{K} \qquad (9)$$

Taking the spurious resonance frequency to be f_{sn} (n=1,2,3, ...) and corresponding θ with θ_{sn} (n=1,2,3, ...), we obtain from (8) and (2)

$$\tan\theta_{s1} = \infty$$
$$\tan^2\theta_{s2} - K = 0$$
$$\tan\theta_{s3} = 0 \qquad (10)$$

Then

$$\frac{f_{s1}}{f_0} = \frac{\theta_{s1}}{\theta_0} = \frac{\pi}{2\tan^{-1}\sqrt{K}}$$
$$\frac{f_{s2}}{f_0} = \frac{\theta_{s2}}{\theta_0} = 2\left(\frac{f_{s1}}{f_0}\right) - 1$$
$$\frac{f_{s3}}{f_0} = \frac{\theta_{s3}}{\theta_0} = 2\left(\frac{f_{s1}}{f_0}\right). \qquad (11)$$

This is one of the special features of the SIR. This structure was developed in coaxial line form and in stripline technology. The main advantages of this structure are :

1. The possibility of controlling spurious responses and insertion losses.
2. The design procedure is independent of the values of the characteristic impedance of the resonators. So, the optimum line dimensions for the maximum unloaded quality factor can be chosen.

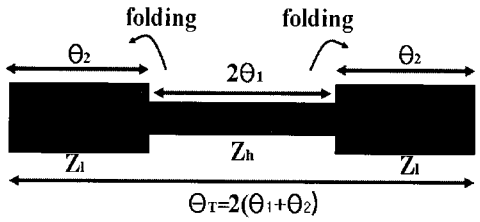

(a)

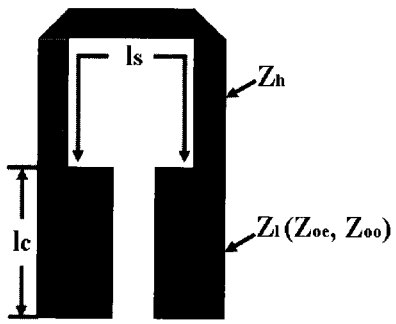

(b)

〈Fig. 1〉 (a) Stepped-impedance resonator and (b) Stepped-impedance hairpin resonator.

3. Design of a Microstrip SIR LPF

Fig. 2 shows the geometry and the equivalent circuit of the low-pass filter without aperture using microstrip stepped-impedance hairpin resonator with feed lines L_f. As it can be seen from the equivalent circuit in Fig. 2(b), L_s and C_s are the equivalent inductance and capacitance, respectively of the single transmission line of the filter. C_g is the equivalent capacitance of the coupled lines and C_p is the equivalent shunt capacitance. Fig. 2(d) shows the equivalent circuit for the filter without aperture, where $C_{ps} = C_s + C_P + C_\Delta$. Here, C_s is the capacitance related to the single transmission line, C_p is the shunt capacitance related to l_c, and C_Δ is the capacitance related to the junction discontinuity between single transmission line and coupled lines.

The microstrip stepped-impedance hairpin resonator with aperture structure to be considered here is shown layout and equivalent circuit in Fig. 3. $L_s^{'}$ is the equivalent inductance of the single transmission line. $C_g^{'}$ is the equivalent capacitance of inter-digital capacitor coupled lines and $C_p^{'}$ is the shunt capacitance related to l_c,

Using aperture on the ground, the single transmission line can be got rid of parasitic capacitance of and harmonic resonances. Also, adopting the inter-digital structure inside the coupled line section, very sharp skirt characteristic in frequency response can be obtained and the size of the device can be reduced.

The conformal mapping technique is used to evaluate closed form expressions for computation of capacitances of IDC on two-layered substrates. The derivation is based on the partial capacitance method and takes into account

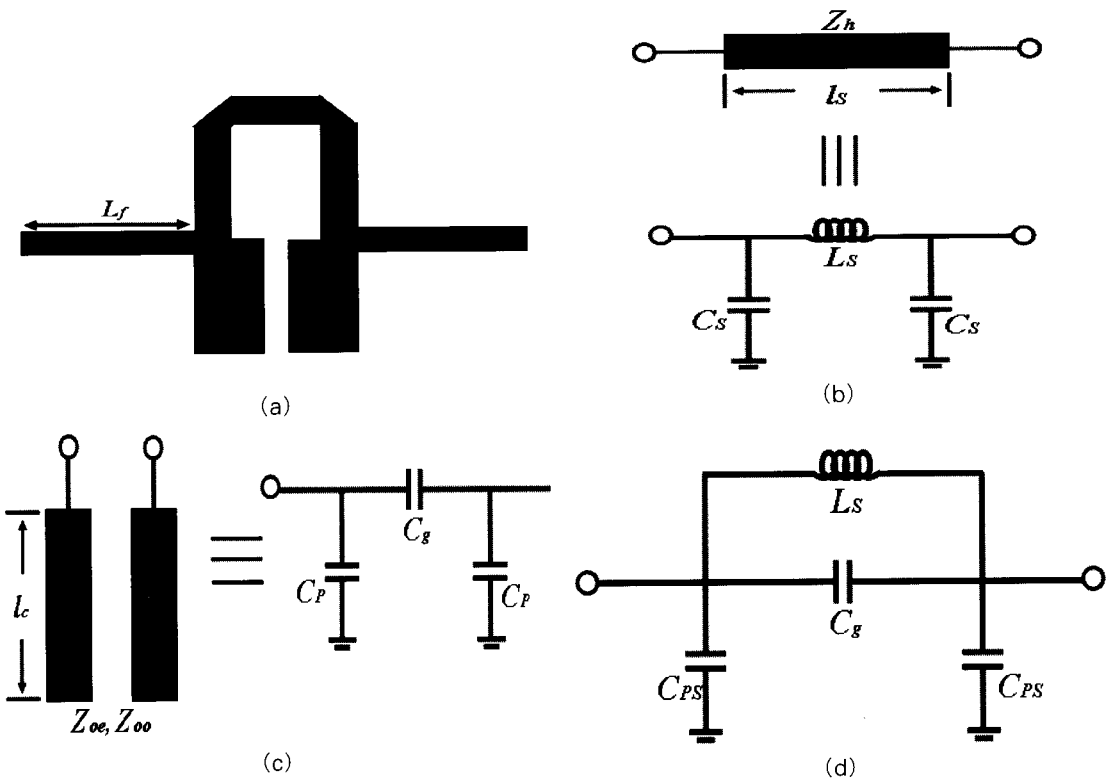

〈Fig. 2〉 Stepped-impedance hairpin resonator low-pass filters without aperture: (a) Layout (b) Equivalent circuit of single transmission lines, (c) Equivalent circuit of symmetric coupled lines, and (d) Equivalent circuit of low-pass filter using one hairpin resonator

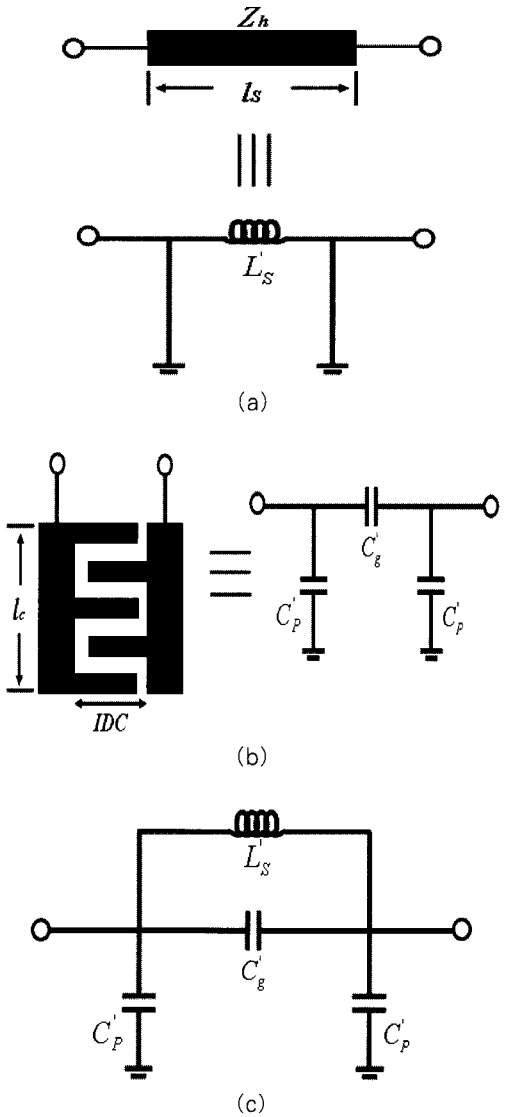

〈Fig. 3〉 Stepped-impedance hairpin resonator low-pass filters with aperture: (a) Equivalent circuit of single transmission lines, (b) Equivalent circuit of symmetric IDC coupled lines, and (c) Equivalent circuit of low-pass filter using one hairpin resonator

the capacitance between the fingers and the fringing capacitance of the finger ends.

The capacitance of inter-digital capacitance (IDC) with $n \geq 3$ structure inside the coupled line section may be presented as $\sum C = C_3 + C_n + C_{end}$, where C_3 is the sum of the capacitance of three-finger capacitor, C_n is the capacitances of periodical *(n-3)* structures, and C_{end} is a correction term for the fringing fields of the ends of the strips, which are given by [8]

$$C_3 = 4\epsilon_0\epsilon_{e3}\frac{K(k_{03})}{K(k_{03}')}l \tag{12}$$

$$C_n = (n-3)\epsilon_0\epsilon_{en}\frac{K(k_{0n})}{K(k_{0n}')}l \tag{13}$$

$$C_{end} = 4ns(2+\pi)\epsilon_0\epsilon_{end}\frac{K(k_{0end})}{K(k_{0end}')} \tag{14}$$

Here, ϵ_0, ϵ_{e3}, ϵ_{en}, and ϵ_{eend} are the dielectric constant in air, the effective dielectric constant with n=3, $n \geq 3$, and of the ends of the finger, respectively. l is the length of finger, n is the number of finger, and s is the width of the finger. *K(k)* and *K(k')* are the modulus of the elliptic integrals of the first kind.

It is assumed that the microwave wavelength in the substrate is much larger than the dimensions of the IDC. The models do not take into account parasitic inductances and resistances.

Using aperture, the single transmission line is modeled as an equivalent inductance π-network, as shown in Fig. 3(a). For the lossless single transmission line with a length of l_s, the *ABCD* matrix is given by

$$\begin{bmatrix} A & B \\ C & D \end{bmatrix} = \begin{bmatrix} \cos(\beta_s l_s) & jZ\sin(\beta_s l_s) \\ jY_s\sin(\beta_s l_s) & \cos(\beta_s l_s) \end{bmatrix} \tag{15}$$

where β_s and $Y_s = 1/Z_s$ are the phase constant and characteristic admittance of the single transmission line, respectively. The *ABCD* matrix of the equivalent inductance π - network is

$$\begin{bmatrix} A & B \\ C & D \end{bmatrix} = \begin{bmatrix} 1+Z_L & Z_L \\ 2+Z_L & 1+Z_L \end{bmatrix} \tag{16}$$

where $Z_L = jwL_s'$ is the angular frequency, and L_s' is

the equivalent inductance of the single transmission line.

Comparing (15) and (16), the equivalent $L_s^{'}$ can be obtained as

$$L_s^{'} = \frac{Z_s \sin(\beta_s l_s)}{w} \, (H) \tag{17}$$

Moreover, as seen in Fig. 3(b), the symmetric parallel inter-digital capacitor coupled lines are modeled as equivalent capacitive π- network. The ABCD matrix of the lossless parallel coupled line is expressed as [16].

$$\begin{bmatrix} A & B \\ C & D \end{bmatrix} = \begin{bmatrix} \frac{Z_{oe}+Z_{oo}}{Z_{oe}-Z_{oo}} & \frac{-j2Z_{oe}Z_{oo}\cot(\beta_c l_c)}{Z_{oe}-Z_{oo}} \\ \frac{j2}{(Z_{oe}-Z_{oo})\cot(\beta_c l_c)} & \frac{Z_{oe}+Z_{oo}}{Z_{oe}-Z_{oo}} \end{bmatrix} \tag{18}$$

where β_c is the phase constant of the coupled lines. Also, the ABCD matrix of the equivalent capacitive π-network is

$$\begin{bmatrix} A & B \\ C & D \end{bmatrix} = \begin{bmatrix} 1+Z_g Y_p & Z_g \\ Y_p(2+Z_g Y_p) & 1+Z_g Y_p \end{bmatrix} \tag{19}$$

where $Z_g = 1/jwC_g^{'}$ and $Y_p = jwC_p^{'}$. In comparison with (18) and (19), the equivalent capacitances of the π-network are found as

$$C_g^{'} = \frac{Z_{oe}-Z_{oo}}{2wZ_{oe}Z_{oo}\cot(\beta_c l_c)} \, (F) \tag{20a}$$

and

$$C_p^{'} = \frac{1}{wZ_{oe}\cot(\beta_c l_c)} \, (F) \tag{20b}$$

The physical dimension of the filter can be synthesized by using the ABCD matrix. The widths of the single transmission line and coupled lines of the filter can be obtained from selecting the impedances that satisfy the condition $Z_h > \sqrt{Z_{0e}Z_{0o}}$. The lengths of the single transmission line and coupled lines of the filter transformed from (17) and (20a) are

$$l_s = \frac{\sin^{-1}(w_c L_{st}/Z_s)}{\beta_s} \tag{21a}$$

and

$$l_c = \frac{\tan^{-1}[w_c Z_{oe}(C_{pt}-C_s)]}{\beta_c} \tag{21b}$$

where w_c is the 3-dB cutoff angular frequency, and L_{st} and C_{pt} are the inductance and capacitance chosen from the ABCD matrix. $C_g^{'}$ can be calculated (20a). Fig. 4 shows the geometry and SEM photograph of the SIR hairpin LPF with aperture and Fig. 5 is the SEM picture of the area of dielectric post. The SIR LPF with aperture on GaAs substrate, in which rectangular shape of defected pattern is etched off from the ground plane, is designed using 3-D simulation tool, HFSS, ver. 8.5. The low-pass filter is designed for 3-dB cutoff frequency of 33 GHz and fabricated on GaAs substrate. The optimized dimensions of the SIR LPF are L_f = *0.5 mm*, L_1 = *0.698 mm*, L_2 = *0.208 mm*, L_3 = *0.26 mm* W_1 = *0.044 mm*, W_2 = *0.044 mm*, W_3=*0.044 mm*, W_4 = *0.04 mm*, W_5 = *0.03 mm*, g = *0.01 mm and* g_1 = *0.01 mm.*

The signal line of DAML structure is consisted of ground metal, dielectric post, and signal line elevated on air. The proposed DAML structure is formed on a GaAs substrate with the thickness of 680 μm, and the ground metal of Au with the thickness of 1 μm while the transmission line has the thickness of 5 μm which is lifted on 10 μm from the ground metal .

4. Process of DAML Structure

The signal line of DAML structure is consisted of

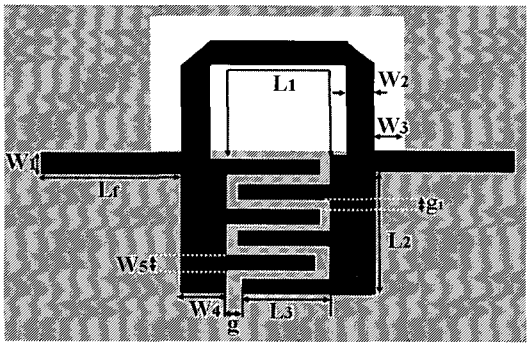

(a)

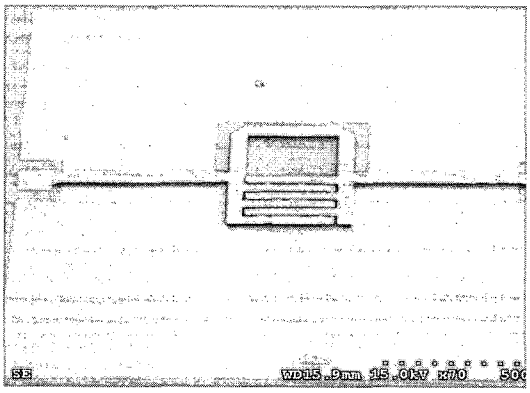

(b)

〈Fig. 4〉 The SIR LPF with aperture. (a) Layout and (b) SEM photograph

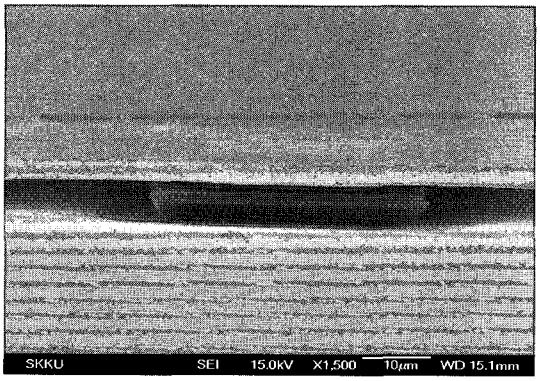

〈Fig. 5〉 SEM photography of the post area

ground metal, dielectric post, and signal line lifted on air. Fig. 5 shows the process flow of the DAML structure using surface micromachining.

First, Ti/Au layer by thermal evaporator [Fig. 6(a)] is deposited on the semi-insulating GaAs substrate, and then

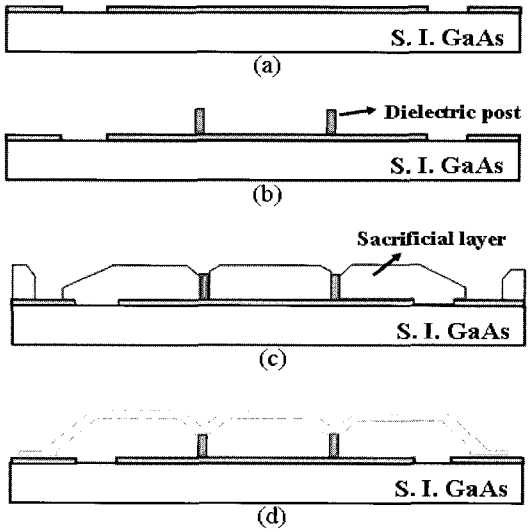

〈Fig. 6〉 Process flow of DAML structure [4] (a) Ground metal formation, (b) Dielectric post formation, (c) Sacrificial photo-resist patterning and baking, and (d) Metal patterning and sacrificial layer removal

the dielectric posts with the height of 10 μm [Fig. 6(b)] are formed. Next, the circuit pattern is finished through the photo-lithography using AZ4903 photo-resist which has higher thickness than post height for the sacrificial layer [Fig. 6(c)]. Finally, the metal pattern can be obtained by lift-off process and the sacrificial layer is removed by acetone [Fig. 6(d)].

5. Simulation and Measurement Results

Fig. 7 shows the simulation and measurement results for the SIR LPFs with and without aperture and IDC. Comparing with each other, the SIR LPF with aperture and IDC shows much broader stopband characteristic, lower return loss, and insertion loss in the pass band, and sharper cutoff frequency than the SIR LPF without aperture and IDC. From the figure, the SIR low-pass filter with aperture shows a 3-dB passband from dc to 33 GHz. The insertion loss is less than 0.82 dB, and the return loss

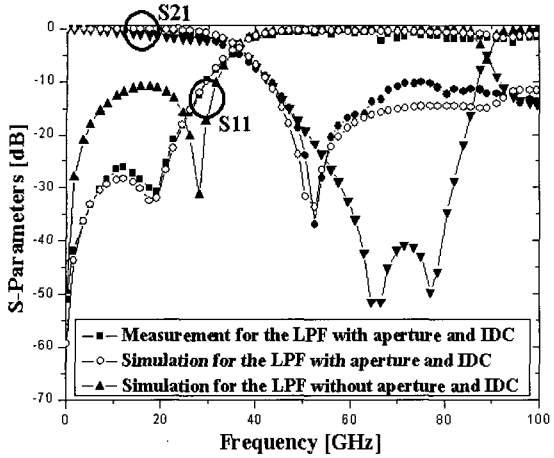

〈Fig. 7〉 Simulation and measurement results for the SIR LPF with aperture and IDC, and without aperture and IDC

is better than 17 dB from dc to 25.57 GHz. The rejection is greater than 10 dB within 43.05-100 GHz. The ripple is ±0.42 dB, as shown in the figure.

6. Conclusions

In this paper, a new millimeter-wave microstrip stepped-impedance hairpin resonator low-pass filter with aperture using GaAs surface micromachining has been proposed. The low-pass filter has shown a sharp cutoff frequency response and low insertion loss. Moreover, with aperture, the low-pass filter shows a wide stopband bandwidth. The experimental results show excellent agreements with theoretical simulation ones.

Acknowledgment

This work was supported by Korea Science and Engineering Foundation (KOSEF) under the Engineering Research Center (ERC) program through the Millimeter-wave INnovation Technology (MINT) research center at Dongguk University.

References

[1] G. M. Rebeiz, *RF MEMS Theory Design and Technology*, Wiley Inter-Science, 2003.

[2] J. De Hector, *RF MEMS Circuit Design*, Artech House, 2002.

[3] H. Henri, S. Gonzague, V. Matthieu, C. Alain, and D. Gilles, "Ultra Low Loss Transmission Lines on Low Resistivity Silicon Substrate," *IEEE MTT-S Int. Microwave Symp. Dig.*, vol. 3, pp. 809-1812, 2000.

[4] H. S. Lee, D. H. Shin, S. C. Kim, B. O. Lim, T. J. Baek, B. S. Ko, Y. H. Chun, S. K. Kim, H. C. Park, and J. K. Rhee,"The Fabrication of the Low Loss Transmission Line and Low Pass Filter Using Surface Microelectromechanical Systems Technology," *Jpn. J. Appl. Phys.*, vol. 43, no. 5A, pp. 2786-2790, 2004.

[5] M. Makimoto and S. Yamashita, Microwave Resonators and Filters for Wireless Communication Theory, Design and Application, Belin, Germany: Spinger-Verlag, Ch. 4, 2001.

[6] M. Sagawa, K. Takahashi, and M. Makimoto, "Miniaturized Hairpin Resonator Filters and Their Application to Receiver Front-end MIC's," *IEEE Trans. Microwave Theory Tech.*, vol. 37, no. 12 , pp. 1991-1997, Dec. 1989.

[7] J. W. Sheen, "A compact semilumped low-pass filter for harmonics and spurious suppression," *IEEE Microwave Guided Wave Lett.*, vol. 10, pp.92-93, Mar. 2000.

[8] J. H. Cho, T. S. Yun, K. B. Kim, J. G. Park, and J. C. Lee, "A Microstrip Stepped-Impedance Hairpin Resonator Lowpass Filter Using Aperture," *Proc. KICS Summer Conf.*, vol. 29, pp. 318- , 2004. 7.

[9] S. S. Gevorglan, T. Martinsson, P. L. Jlinner, and E. L. Kollberg,"CAD Models for Multilayered Substrate Interdigital Capacitors", *IEEE Trans. Microwave Theory Tech.*, vol 44, pp. 896-904, 1996.

〈저자소개〉

조 주 현 (Ju-Hyun, Cho)
2003년 2월 : 강남대학교 전자공학부(공학사)
2003년 2월~현재 : 광운대학교 전파공학과 공학석사과정

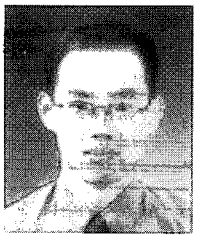

윤 태 순 (Tae-Soon, Yun)
2000년 2월 : 국민대학교 전자공학과(공학사)
2002년 2월 : 광운대학교 전파공학과(공학석사)
2002년 3월~현재 : 광운대학교 전파공학과 박사과정

고 백 석 (Tae-Jong, Baek)
2003년 2월 : 동국대학교 전자전기공학부(공학사)
2003년 3월~현재 : 동국대학교 대학원 전자공학과 공학석사과정

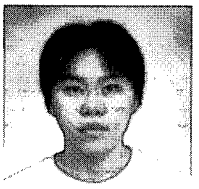

백 태 종 (Baek-Seok, Ko)
2003년 2월 : 중부대학교 정보통신공학과(공학사)
2003년 3월~현재 : 동국대학교 전자공학과 공학석사과정

신 동 훈 (Dong-Hoon, Shin)
1982년 : 동국대학교 물리학과 (공학사)
1984년 : 동국대학교 물리학과 (공학석사)
1999년 : 런던대학교 전기전자공학과 (공학박사)
1999년~현재 : 동국대학교 밀리미터파 신기술 연구센터 연구교수

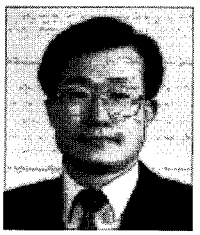

이 종 철 (Jong-Chul, Lee)
1983년 2월 : 한양대학교 전자공학과 (공학사)
1985년 2월 : 한양대학교 전자공학과 (공학석사)
1989년 12월 : Arizona State Univ. EE Dept. (공학석사)
1994년 5월 : Terxas A&M UNiv. EE Dept. (공학박사)
1994년 6월~1996년 2월 : 현대전자 광소자 개발실(선임연구원)
1996년 3월~현재 : 광운대학교 전파공학과 전임강사/조교수/부교수